

Muffler Internal Geometry Parametric Study Related to Sound Transmission Loss and Pressure Drop

Mahadhir Mohammad¹, Mohd Farid Muhamad Said^{2*} & Srithar Rajoo¹

¹UTM Center for Low Carbon Transport (LOCARTIC)
School of Mechanical Engineering, Faculty of Engineering,
Universiti Teknologi Malaysia, 81310 UTM Johor Bahru, Johor,
Malaysia

²Automotive Development Centre (ADC)
School of Mechanical Engineering, Faculty of Engineering,
Universiti Teknologi Malaysia, 81310 UTM Johor Bahru, Johor,
Malaysia

Article history

Received
26th July 2021
Revised
14th October 2021
Accepted
20th December 2021
Published
25th December 2021

*Corresponding email: mdfarid@utm.my

ABSTRACT

A muffler is a device used to attenuate noise generated in an exhaust system. The current research objective is to study the changes in internal muffler geometry effect towards the sound transmission loss (STL) and pressure drop (PD). A complex muffler of 1.6L natural aspirated engine was chosen for this research work. The research tools used were Ricardo Wave Build and Wave Build 3D. The four focus parameters: main muffler volume, pipe diameter, porosity of the baffle and porosity of the inlet pipe. The effect of internal geometry was analysed from the parametric studies. When the muffler volume increased by 10%, the average STL increased by 1% and the PD reduced by 2% respectively. When the diameter of the pipe increased with fixed muffler volume, the average STL dropped by 9% and PD dropped by 30%. The perforated on baffle showed less effect on average STL which can increase by a maximum of 1 dB and PD showed an average reduction by 0.8% as the perforated on baffle increased. For the case of perforated on pipe, as perforated on pipe increase, STL improved less than 1dB and PD reduced by 7%. From the result of all parametric studies, the STL was mostly affected by the muffler main volume while PD was affected by the pipe diameter.

Keywords: *muffler, sound transmission loss, pressure drop, exhaust, 1D simulation*

1.0 INTRODUCTION

Despite the high demand of technology in plug in hybrid vehicle (PHEV) or hybrid electric vehicle (HEV), the internal combustion engine (ICE) still widely used as power unit for automotive sector. Hence, muffler is a compulsory device to attenuate the noise generated from the engine. Muffler can be divided into two types: reactive muffler and dissipative muffler [1]. Reactive muffler principle operation, the sound wave was attenuated between incident and reflective wave. For dissipative muffler principle operation, the sound wave was absorbed by the absorption material such as wool or fibre. Nowadays, common vehicle uses hybrid muffler consists of reactive and dissipative muffler. In current technologies, the muffler has become an active device to control the noise level [2].

Reactive muffler noise attenuation governs by the parameter of muffler internal geometry [3]. The parameter such as main muffler volume, pipe diameter, perforated on

pipe, pipe length, baffle spacing and perforated on baffle, affects the muffler's performances on sound transmission loss (STL) and pressure drop (PD). Reactive muffler is commonly used to decrease flow noise in duct or pipes of mechanical system [4]. Muffler volume corresponds to muffler's length and radius. An expansion chamber (no internal geometry) was used to study the effect of STL by varying nine different configuration of muffler length from 0.205 cm to 3.525 cm with fixed diameter were studied. The frequency range is up to 3000 Hz. From the studies, if the chamber length shortens, the frequency range become very narrow. Furthermore, the short chamber act like a resonator rather than broadband behaviour [5]. Advanced muffler with adjustable chamber length also reliable to control noise at certain frequency level [6].

Baffle plate is another geometry inside muffler that can enhances the STL. Presence of baffle plate with different positioning or distance shifts the peak of the STL to the left of right of the graph [7]. However, the baffle plat increases the pressure drop across muffler. To minimise the pressure drop, multiple hole was introduced into the baffle plate [8]. However, multiple holes can dissipate unstable vortex and lead to loss of acoustic energy. This may cause the acoustic resistance increase as the flow through orifice increase [9].

Porosity is holes on baffle plate and pipe. Porosity can be defined as ratio of void surface to total surface area. Porosity governs by the number of holes and the hole diameter. The hole diameter of the perforation and wall thickness of perforated tube do not give significant effect towards STL, it is just ± 1 dB of STL. Furthermore, the diameter range cover for this study only 3.0 mm, 4.0 mm and 5.0 mm only [10]. Perforated pipe has high impact on high frequency range, above 400 Hz [11]. The hole's diameter is effective to attenuate noise at low frequency starting from 3.0 mm to 7.0 mm [12]. Pressure drops and STL will increase when the diameters, perforated ratio and length of perforated decreased [13]. Having larger hole diameter can reduce the pressure drop [14].

From the literature review, it can be seen there are still lack of studies in the muffler internal geometry parameter. Most of the studies using a simple geometry muffler while in this study using a commercial muffler with various geometry inside the muffler. Furthermore, the scope of the study for each parameter also limited to a certain range. Hence the research objective is to study the changes in internal muffler geometry effect towards the sound transmission loss (STL) and pressure drop (PD). Four parameters were focused, main muffler volume, pipe diameter, perforated on baffle and perforated on pipe.

2.0 METHODOLOGY

In this section, the methodology highlights the use of 1D software to conduct comprehensive parametric study on the complex muffler. Sound transmission loss (STL) and pressure drop (PD) were measured to quantify the muffler performances. The muffler geometry was already validated with experimental data on the previous research conducted [15]. Ricardo Wave Build and Wave Build 3D were used as simulation tools. The muffler was constructed in Wave Build 3D and then exported into the Wave Build.

2.1 Sound Transmission Loss (STL)

STL simulation was conducted using Ricardo Software. The 3D model was developed using Ricardo Wave Build 3D and then the 3D model exported to Ricardo Wave Build to run the simulation. Figure 1 shows the simulation setup to measure the sound transmission loss.

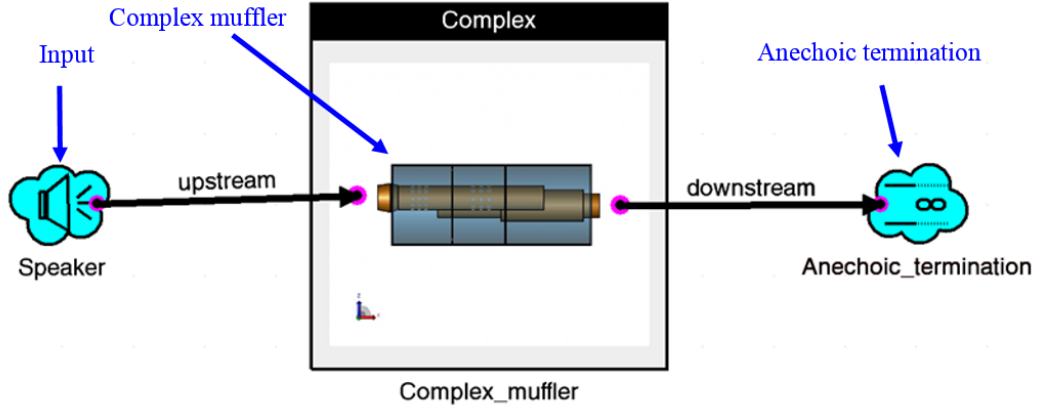


Figure 1: Simulation setup for sound transmission loss (STL)

A speaker (acoustic piston) was set on the upstream while an anechoic termination was stationed at the downstream pipe. The speaker generated a sinusoidal step noise from 10 Hz to 1000 Hz. Four microphones were modelled in the simulation, two microphone on upstream tube and another two at the downstream tube. The upstream length, downstream length and microphone spacing are based on the actual rig used to validate the baseline data. The microphone spacing and length are fixed through all parameters. However, for the parametric study on pipe diameter effect, the upstream and downstream tube diameter is set to follow the pipe diameter. This to avoid any area discontinuity that can affect the STL and PD effects. The initial condition was set on 1.0 bar and 300 K. The physical properties were defined as Table 1 and muffer meshing was defined as Table 2.

Table 1: Specimen physical properties for STL

Properties	Complex muffer
Friction multiplier	1
Heat transfer multiplier	1
Pressure loss coefficient	0
Wall temperature	300 K

Table 2: Muffer meshing size

Axis	Complex muffer (mm)
dx	18.0
dy	24.0
dz	29.0

STL was computed using transfer function method, equation 1 and equation 2. Since the STL curve is function of frequency, average of STL across all frequency had been taken to ease the analysis performance process. Average STL computed using equation 3.

$$T = \begin{bmatrix} T_{11} & T_{12} \\ T_{21} & T_{22} \end{bmatrix} = \begin{bmatrix} \frac{p_{0a} u_{db} - p_{0b} u_{da}}{p_{da} u_{db} - p_{db} u_{da}} & \frac{p_{0b} p_{da} - p_{0a} p_{db}}{p_{da} u_{db} - p_{db} u_{da}} \\ \frac{u_{0a} u_{db} - u_{0b} u_{da}}{p_{da} u_{db} - p_{db} u_{da}} & \frac{p_{da} u_{0b} - p_{db} u_{0a}}{p_{da} u_{db} - p_{db} u_{da}} \end{bmatrix} \quad (1)$$

$$STL = \left[\frac{T_{11} + \left(\frac{T_{12}}{\rho c} \right) + \rho c T_{21} + T_{22}}{2e^{ikd}} \right] \quad (2)$$

$$\text{Average } STL = \frac{\sum STL}{N} \quad (3)$$

2.2 Pressure Drop (PD)

Another important muffler performance is pressure drop (PD). PD is a very crucial parameter in the exhaust system. Higher PD causes the engine volumetric efficiency drop. Figure 2 shows the setup to measure the pressure drop of the muffler. An airflow input was set at the upstream. Boundary condition for downstream was define as room conditions Two pressure transducers were predefined at the upstream and downstream duct.

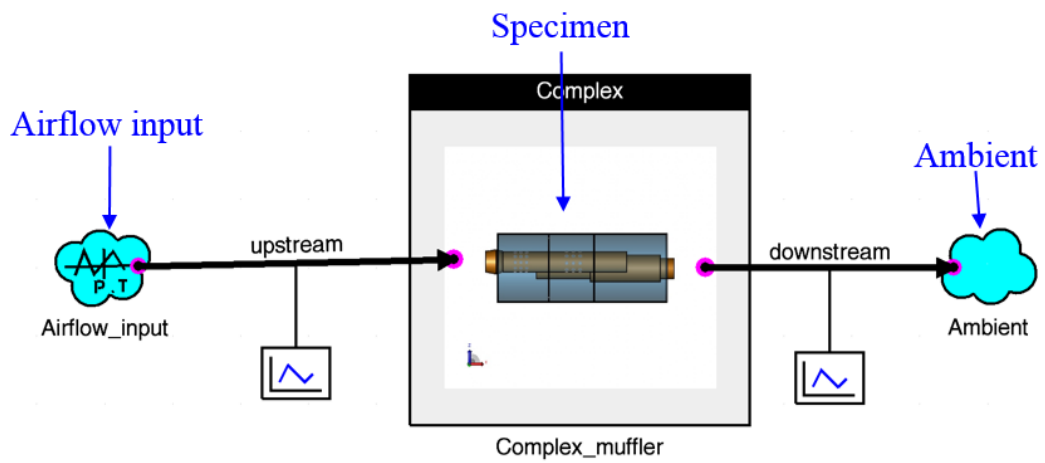


Figure 2: Simulation setup for pressure drop

The air flow input equivalent to 1.6 natural aspirated (NA) engine at wide open throttle (WOT) conditions, 1000 RPM to 6000 RPM [16]. One of the most important parameters for the PD simulation is pressure loss coefficient (PLC). To measure the PLC, an experiment was conducted. The experiment was conducted on SuperFlow bench tests shown in Figure 3. Magnitude of the PLC was calculated using equation 4 and PD performances was computed using equation 5. PD simulation input is mass flow rate and PLC magnitude is as shown in Table 3.

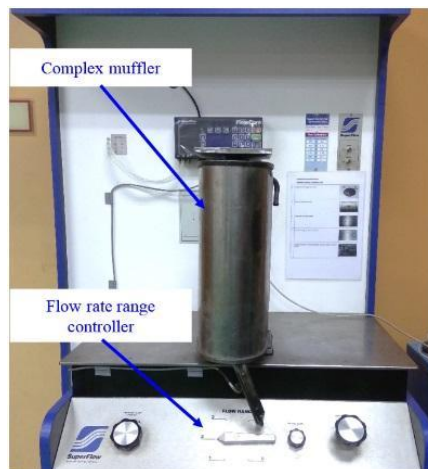


Figure 3: Complex muffler mounted on SuperFlow test bench

$$\xi = \frac{2 \Delta p}{\rho_a V_a^2} \quad (4)$$

$$\Delta P = P_{upstream} - P_{downstream} \quad (5)$$

Table 3: Input mass flow and PLC coefficient

CFM	Mass flow (kg/s)	PLC
30	0.014	0.69
50	0.023	0.64
70	0.032	0.32
90	0.042	0.31
110	0.051	0.22
130	0.061	0.21
150	0.072	0.20

2.3 Parametric Studies

Parametric studies were carried to identify the internal geometry effect towards the STL and PD. Figure 4 shows the four parameters of muffler internal geometry focusing on, main muffler volume (a), pipe diameter (b), perforated on baffle (c), and perforated on pipe (d).

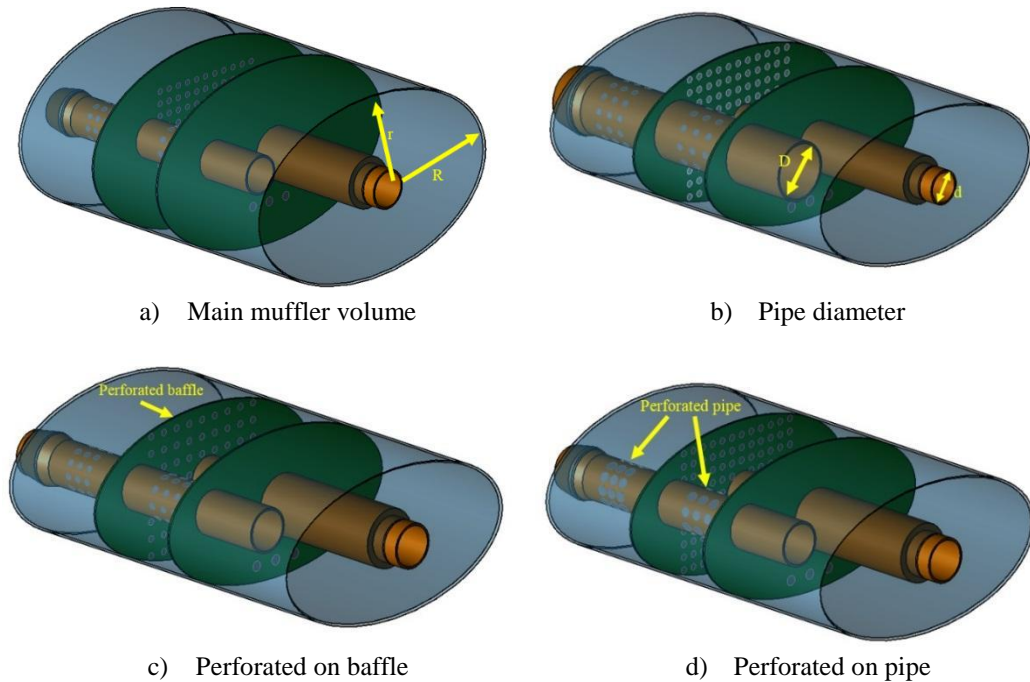


Figure 4: Four muffler parameters and its label

All parameters were changed in Wave Build 3D and were exported to Wave Build. Main muffler volume varied according to the major radius (R) and minor radius (r) as shown in Figure 4a. The muffler length was fixed. The variation of the main muffler volume is as shown in Table 4. Pipe diameter (D and d) as shown in Figure 4b were changed accordingly with increment and decrement of 5.0 mm and the range is from

30.0 mm to 55.0 mm. The pipe diameter's original size (baseline) is 40.0 mm, same for the inlet and outlet. Table 5 shows the pipe diameter parameter size.

For the perforated on baffle, its divided into two categories, which are number of holes and hole diameter. Figure 4c shows the section perforated on baffle. Table 6 shows the cases for the perforated on baffle parameter.

Last parameter is perforated on pipe. For perforated on pipe divided into two categories, which are number of holes and hole diameter. Figure 4d shows the section perforated on pipe. Table 7 shows the cases perforated on pipe.

Table 4: Main muffler volume parameter

Case	Volume (L)	Major Radius (mm)	Minor Radius (mm)
Baseline	11.40	140	172
1	9.12	130	62
2	10.23	135	67
3	12.63	145	77
4	13.91	150	82
5	16.65	160	92
6	19.61	170	102
7	22.80	180	112
8	28.01	195	127

Table 5: Pipe diameter parameter

Case	Inlet diameter, D (mm)	Outlet diameter, d (mm)
Baseline	40	40
9	30	30
10	35	35
11	45	45
12	50	50
13	55	55
14	30	55
15	55	30

3.0 RESULTS AND DISCUSSION

3.1 Main muffler volume effect

Figure 5a shows the result of volume effect towards sound transmission loss. From all cases, four cases result were plotted to show the volume effect. The smallest volume is Case 1, 9 L and the biggest volume is Case 8, 28 L. Case 1 curve shows the lowest sound attenuation between 160 Hz to 550 Hz. Case 8, the biggest volume, has the highest sound attenuation occur from 90 Hz to 380 Hz and 660 Hz to 840 Hz. However, at the biggest volume, no maximum amplitude occurs. The maximum sound attenuation is 50 dB occur at 620 Hz, Case 2 (9 L) and 450 Hz, Case 6 (20 L). Since it is hard to see the overall performance under 1000 Hz, an average STL was used to determine the overall effect. The sum of all STL magnitude is divided by the total point. Figure 5b shows the average STL versus muffler volume. From Figure 5b, a conclusion can be drawn. The higher muffler volume, the higher the STL. This conclusion can be achieved if the internal geometry parameter was fixed.

Figure 5c shows the muffler PD versus muffler volume. At a constant volumetric flow rate, the PD decrease linearly when the muffler volume increase. At 30 CFM constant volumetric flow rate line, when the volume is 9 L, the PD is 3.03 mbar and as the volume increase to 28 L, the PD reduce to 2.72 mbar. At 150 CFM, the PD reduce from 58.33 mbar to 56.67 mbar when the muffler volume from 9 L increase to 28 L.

Table 6: Perforated on baffle parameter

Case	Hole diameter (mm)	Hole numbers
Baseline	6.5	100
16	6.5	60
17	6.5	70
18	6.5	80
19	6.5	90
20	6.5	110
21	6.5	120
22	6.5	130
23	6.5	140
24	6.5	150
25	6.5	160
26	6.5	170
27	6.5	180
28	6.5	190
29	6.5	200
30	2.5	100
31	3.5	100
32	4.5	100
33	5.5	100
34	7.0	100
35	7.5	100
36	8.5	100
37	9.0	100
38	9.5	100
39	10.0	100
40	10.5	100
41	11.0	100

Average reduction of PD when the muffler volume increase is 5.3%. This result was supported by other researcher stated that the muffler PD increase when the muffler size is reduced without changing number of holes in inlet and outlet pipes and baffle positions [17].

3.2 Pipe diameter effect

Figure 6a shows the result of pipe diameter effect towards STL. The baseline pipe diameter is 40.0 mm. Case 14 shows that the inlet diameter is smaller than the outlet while Case 15 shows that the inlet diameter is larger than the outlet. Case 9 displays the smallest pipe diameter with highest attenuation. The range is from 160 Hz to 550 Hz and 750 Hz to 1000 Hz. The largest pipe diameter is 55.0 mm, Case 13, shows the lowest sound absorption ranging from 180 Hz to 1000 Hz, consistently the lowest sound

attenuation. Case 14's sound attenuation maximum amplitude is at 570 Hz, 33 dB, while Case 15 has sound attenuation maximum amplitude at 610 Hz, 54 dB.

Figure 6b shows the average STL versus cases number. The cases number correspond to the pipe diameter. Case 9 has the smallest pipe diameter, 30.0 mm with the highest average of STL. Case 13 has the largest pipe diameter, 55.0 mm with the lowest sound absorption level. A conclusion can be drawn in which the smaller the pipe diameter, the higher the STL and vice versa.

Table 7: Perforated on pipe parameter

Case	Hole diameter (mm)	Hole numbers
Baseline	6.5	30
42	6.5	10
43	6.5	15
44	6.5	20
45	6.5	25
46	6.5	35
47	6.5	40
48	6.5	45
49	6.5	50
50	3.0	30
51	4.0	30
52	5.0	30
53	6.0	30
54	7.0	30
55	8.0	30
56	9.0	30
57	10.0	30

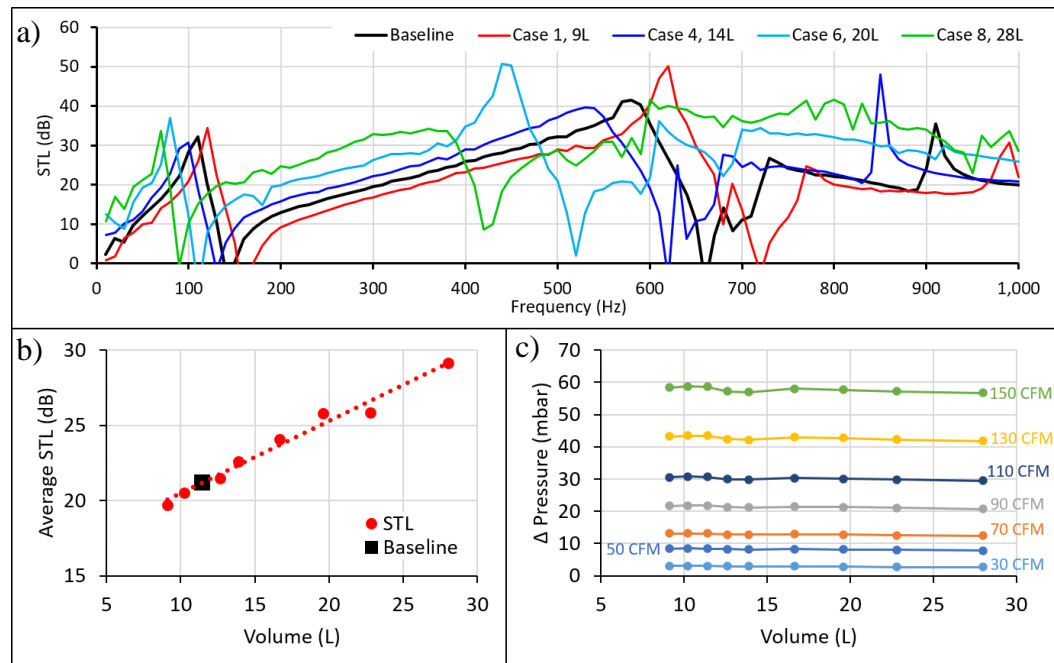


Figure 5: Volume effect towards STL and pressure drop; a) STL versus frequency curve; b) Average STL versus muffler volume; c) Pressure drop versus muffler volume

Case 14's STL is significantly same with Case 11 and same goes with case 15's STL with Case 10. By having a bigger inlet pipe and smaller outer pipe, the average STL increase by 7%. On the other hand, having bigger outlet pipe, reduce the average of STL.

Figure 6c shows the PD versus pipe diameter. A large volume flow rate, 150 CFM with small pipe, contribute to high PD. The upstream pressure was higher than the downstream. The flow was restricted because of the small flow area. By increasing the pipe diameter, the PD of the large volume flow rate can be reduced from 214 mbar at 30.0 mm, to 26 mbar at 55.0 mm. This trend is shown in Figure 6c. However, for the smaller volume flow rate at 30 CFM, the PD decreased as the pipe diameter increase, compared to the large volume flow rate. Figure 7 shows the PD result for Case 14 and Case 15. If the outlet diameter is small like Case 15, the PD is higher than the small inlet diameter. Meanwhile, Case 14 with larger outlet pipe is significantly same with the baseline model.

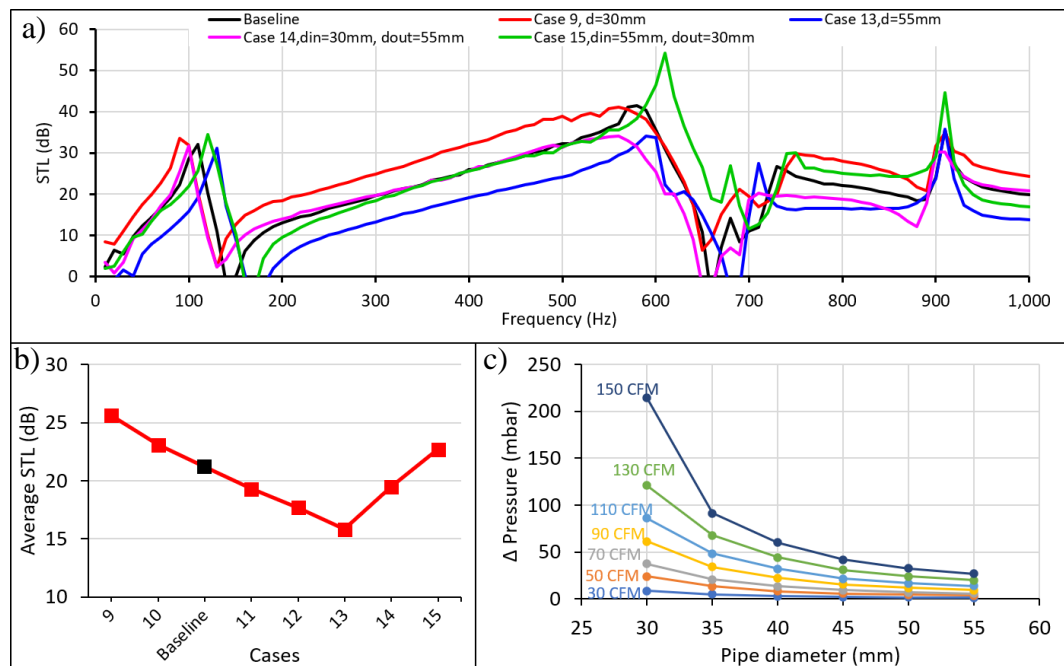


Figure 6: Pipe diameter effect towards STL and pressure drop; a) STL versus frequency curve; b) Average STL versus cases number; c) Pressure drop versus pipe diameter

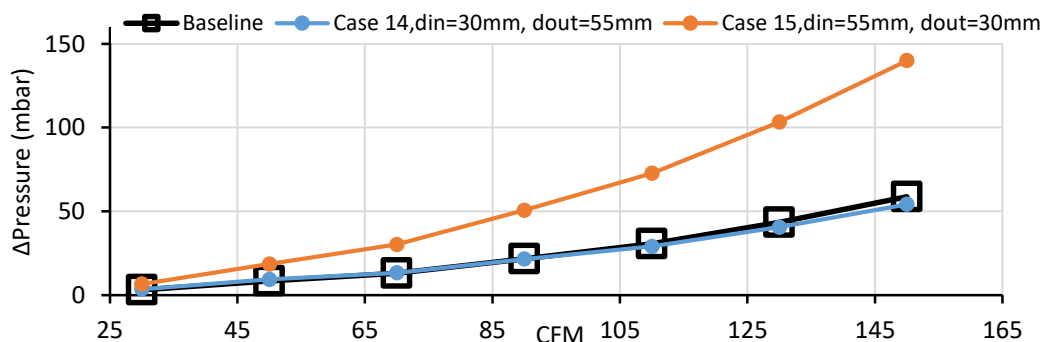


Figure 7: Muffler pressure drop for Case 14 and Case 15

3.3 Perforated on baffle

Figure 8a shows the result of perforated on baffle based on the number of holes effect towards STL. This parameter focus on increased and decreased the number only, the hole arrangement was fixed for all hole numbers. In Case 22, 130 holes have maximum amplitude 70 dB of STL at 610 Hz. The baseline maximum amplitude is only 41 dB at 570 Hz. Case 22's STL is 70% higher than the baseline, this means more noise was attenuated with increase of numbers of hole. The perforated on baffle STL effects mostly between 500 Hz to 710 Hz. Case 16, with the least numbers of hole (60 holes), makes the maximum amplitude shift towards the left side of the curve and achieved the maximum attenuation early than larger number of holes. However, from Case 23 to Case 29, the maximum amplitude drops from 70 dB to 39 dB and they are lower than the baseline result. This indicate the number of holes has its optimum value, because as the number of holes increase from Case 23 to Case 29, the STL consequently.

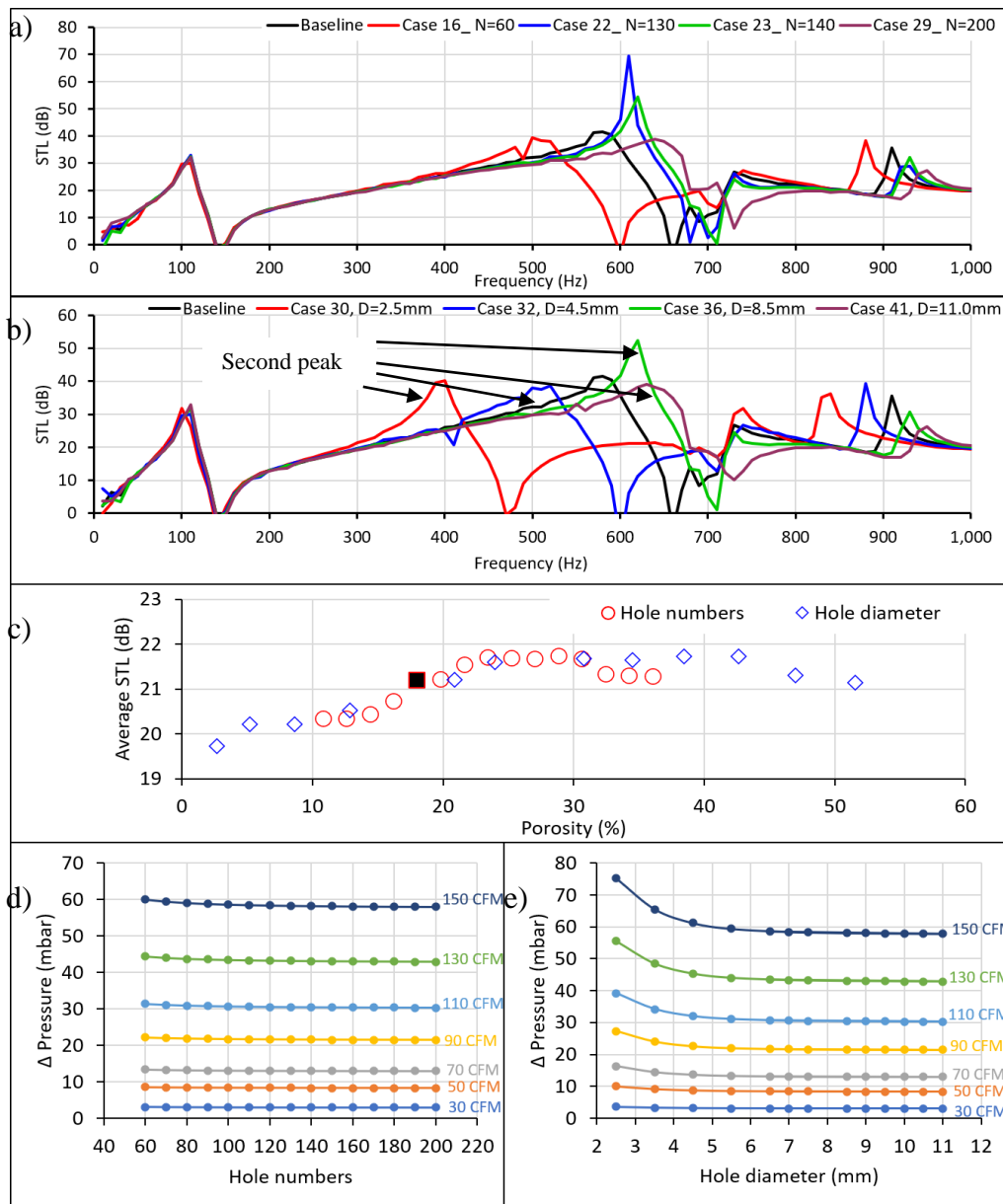


Figure 8: Perforated on baffle effect towards STL and pressure drop; a) STL versus frequency curve hole number effect; b) STL versus frequency curve hole diameter effect; c) Average STL

versus perforated on baffle porosity; d) Pressure drop versus hole numbers on baffle; e) Pressure drop versus hole diameter on baffle

Figure 8b shows the result of perforated on baffle based on hole diameter effect towards STL. The maximum STL occurs at Case 36, frequency 620 Hz at magnitude 52 dB. Case 30, with the smallest hole diameter, peak shift to the very left of the curve and lower the broadband noise coverage. Case 30, Case 32 and 41, the peak amplitudes are significantly the same with the baseline muffler. However, the frequency coverage is difference. Small diameters have lower frequency coverage for the second peak while with the largest diameter, the frequency coverage is wider for the second peak. Second peak is labelled in Figure 8b.

Figure 8c shows the average STL versus porosity on the baffle plate. The average STL of hole number increases from porosity 12% to 23%. After that, the magnitude of average STL maintains from porosity 22% to 30%. Then, the average STL drops from 21.7 dB to 21.3 dB. Same trend happens to the hole diameter effect. However, the diameter can have higher porosity to maintain the average STL from 24% to 43%. After 43%, the STL drops significantly from 21.7 dB to 21.3 dB. Even though the hole diameter and hole number have the same porosity at 12.7%, the average STL difference is 0.88%, less than 1% of difference. At 30% porosity, the average STL magnitude was same for both cases. The average changes of the average STL perforated on baffle is ± 1 dB and this is supported by previous researcher [10].

Figure 8d shows the PD across the muffler versus hole numbers on the baffle plate. The PD increases when volume flow rate increases. Having multiple number of holes, the PD is lower while having less hole, the PD is high. From Figure 8d, at constant CFM 150, the PD was higher when the number of holes less than 100. The PD increase by 0.31% to 2.42%. If number of holes higher than 100, the PD is reduced by 0.24% to 1.09%.

Figure 8e shows the PD across the muffler versus hole diameter in baffle plate. Small hole diameter will have higher PD. When the hole diameter increases, the PD reduces significantly. At 150 CFM, the PD was 75.2 mbar when the diameter is 2.5 mm. When the diameter increases to 11.0 mm, the PD become 57.9 mbar. The changes of reduction PD are 30%. At low flow rate, 30 CFM, the pressure is 3.6 mbar when diameter is 2.5 mm. Apart from that, when the diameter is 11.0 mm, the pressure is only 2.9 mbar. The difference is only 2%. At very low flow rate of 30 CFM, the PD is less significant compared to a high flow at 150 CFM.

3.4 Perforated on pipe

Figure 9a shows the result of perforated on pipe based on the number of hole effect towards STL. Meanwhile, Figure 9b shows the result of perforated on pipe based on hole diameter effect towards STL. The hole diameter and hole numbers have the same effect towards STL. The maximum STL occurs at 600 Hz. The maximum amplitude occurs with lowest porosity in which both cases show that the maximum amplitude occur with only 10 holes numbers (Case 42) with diameter of 3.0 mm (Case 50). At other frequency, no significant changes identified in STL curve. The STL effect on porosity was very marginal at low frequency compared with high frequency [18].

Figure 9c shows the average STL versus hole porosity. The average STL drops linearly across as the porosity increase. This happens because more noise is able to pass through the perforated hole when the porosity is high.

Figure 9d shows the hole number effect towards PD across the muffler. The least number of holes, Case 42 has a high PD, unlike the Case 49 that has lowest PD. Case 42, the average PD increases by 132.4%, higher than the baseline. Case 49, the average PD decreases by 8.89%, lower than the baseline.

Figure 9e shows the hole diameter effect towards PD across the muffler. The smallest hole diameter has the highest PD while the biggest hole has the lowest PD. This was agreed from previous findings [14]. Case 50, the hole diameter is 3.0 mm and the average PD increases by 358%, higher than the baseline model. Apart from that, Case 57, with 10.0 mm hole diameter, the PD is lowered by 9% from the baseline model. The hole diameter contributes more towards the pressure drop increment rather than the hole numbers. Table 8 shows the summary of the parametric study.

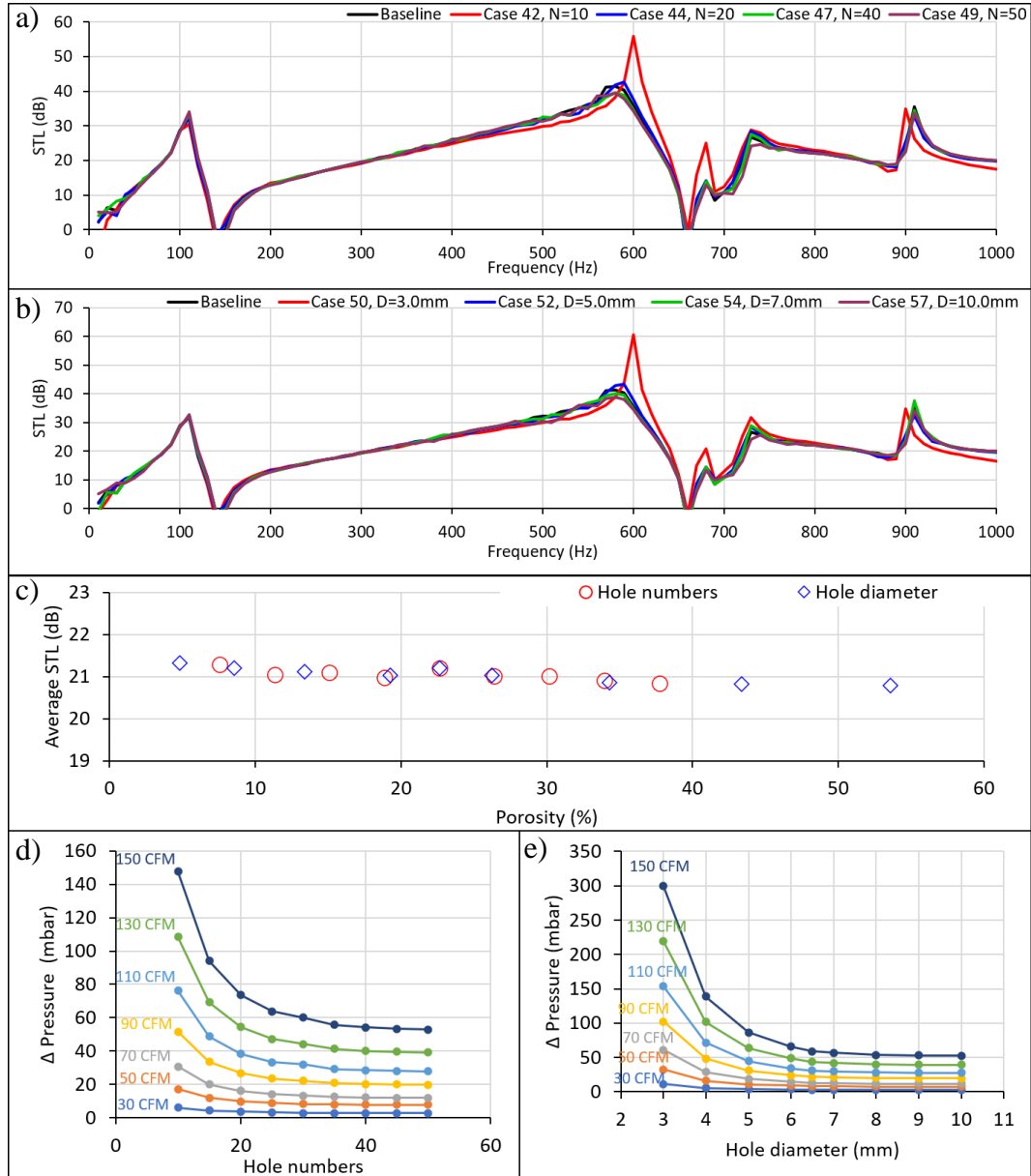


Figure 9: Perforated on pipe effect towards STL and pressure drop; a) STL versus frequency curve hole number effect; b) STL versus frequency curve hole diameter effect; c) Average STL versus perforated on pipe porosity; d) Pressure drop versus hole numbers on pipe; e) Pressure drop versus hole diameter on pipe

Table 8: Summary of the parametric study

Parameter		Average STL	Pressure drop
Volume	Larger volume	Increase	Decrease
	Smaller volume	Decrease	Increase

Pipe diameter	Bigger pipe	Decrease	Decrease
	Smaller pipe	Increase	Increase
Perforated baffle	High porosity	± 1 dB	Significant
	Low porosity	± 1 dB	Significant
Perforated pipe	High porosity	Not significant	Decrease
	Low porosity	Not significant	Increase

4.0 CONCLUSION

In conclusion, the main shell volume, pipe diameter inlet and outlet, perforated on baffle, and perforated on pipe were studied. When the main shell volume increased by 10%, the average STL increased by 1% and the PD reduced by 2% respectively. Reduction pipe diameter by 12%, it increases the average STL by 9% and the average PD increased by 55%. If the pipe diameter increases by 12%, its lower the average STL by 9% and PD reduced by 30%. Perforated on baffle effect the STL by changes the maximum amplitude point and the average STL changes is ± 1 dB only. The PD perforated on baffle reduce by 1.3% at 51% of porosity, which are the maximum porosity. Perforated on pipe STL increase the peak resonance frequency. The average STL of perforated on pipe decrease linearly from 21.29 dB to 20.85 dB as the porosity increase from 7% to 53%. Perforated on pipe can reduce the PD by 10% at maximum porosity, 45%. For future work, the data generated from this research work can use as input data for optimisation work.

ACKNOWLEDGMENTS

The authors would like to acknowledge the Universiti Teknologi Malaysia (UTM) for financial support under the research university grant Q.J130000.2524.17H17.

NOMENCLATURE

STL	Sound transmission loss	p_{0a}	Acoustic pressure at inlet with termination a (anechoic)
N	Number of points	p_{0b}	Acoustic pressure at inlet with termination b (hard end)
P	Pressure	p_{da}	Acoustic pressure at outlet with termination a (anechoic)
ξ	Pressure loss coefficient	p_{db}	Acoustic pressure at outlet with termination b (hard end)
ρ	Density	u_{0a}	Particle velocity at inlet with termination a (anechoic)
V	Velocity	u_{0b}	Particle velocity at inlet with termination b (hard end)
a	Air	u_{da}	Particle velocity at outlet with termination a (anechoic)
T	Transfer matrix	u_{db}	Particle velocity at outlet with termination b (hard end)
ρ	Density	c	Speed of sound
CFM	Cubic feet per minute	WOT	Wide open throttle

REFERENCES

- [1] Ashok Reddy K 2017 A Critical Review on Acoustic Methods & Materials of a Muffler *Materials Today: Proceedings* vol 4 (Elsevier) pp 7313–34
- [2] Drant J, Micheau P and Berry A 2021 Active noise control in duct with a harmonic acoustic pneumatic source *Appl. Acoust.* **176** 107860
- [3] Vijayasree N K K and Munjal M L L 2012 On an Integrated Transfer Matrix method for multiply connected mufflers *J. Sound Vib.* **331** 1926–38
- [4] Lee J W 2015 Optimal topology of reactive muffler achieving target transmission loss values: Design and experiment *Appl. Acoust.* **88** 104–13
- [5] Selamat A and Radavich P M 1997 The effect of length on the acoustic attenuation performance of concentric expansion chambers: An analytical, computational and experimental investigation *J. Sound Vib.* **201** 407–26
- [6] Xiang L, Zuo S, Wu X and Liu J 2017 Study of multi-chamber micro-perforated muffler with adjustable transmission loss *Appl. Acoust.* **122** 35–40
- [7] Kheybari M and Ebrahimi-Nejad S 2018 Locally resonant stop band acoustic metamaterial muffler with tuned resonance frequency range *Mater. Res. Express* **6** 25802
- [8] Elsayed A, Bastien C, Jones S, Christensen J, Medina H and Kassem H 2017 Investigation of baffle configuration effect on the performance of exhaust mufflers *Case Stud. Therm. Eng.* **10** 86–94
- [9] Chen Z, Ji Z and Huang H 2019 Acoustic impedance of perforated plates in the presence of bias flow *J. Sound Vib.* **446** 159–75
- [10] Munjal M L, Krishnan S and Reddy M M 1993 Flow-acoustic performance of perforated element mufflers with application to design *Noise Control Eng. J.* **40** 159–67
- [11] Yedeg E L, Wadbro E and Berggren M 2016 Interior layout topology optimization of a reactive muffler *Struct. Multidiscip. Optim.* **53** 645–56
- [12] Munjal M L 1987 *Acoustics of Ducts and Mufflers With Application to Exhaust and Ventilation System Design* (Canada: John Wiley & Sons)
- [13] Chiu M-C C 2010 Shape optimization of multi-chamber mufflers with plug-inlet tube on a venting process by genetic algorithms *Appl. Acoust.* **71** 495–505
- [14] Panigrahi S N and Munjal M L 2007 Backpressure considerations in designing of cross flow perforated-element reactive silencers *Noise Control Eng. J.* **55** 504–15
- [15] Mohammad M, Muhamad Said M F, Khairuddin M H, A Kadir M K, Dahlan M A A and Zaw T 2020 Complex geometry automotive muffler sound transmission loss measurement by experimental method and 1D simulation correlation *IOP Conference Series: Materials Science and Engineering* vol 884
- [16] Mohammad M, Buang M M A, Dahlan A A, Khairuddin M H and Muhamad Said M F 2017 Simulation of automotive exhaust muffler for tail pipe noise reduction *J. Teknol.* **79**
- [17] Guhan C P O A, Arthanareeswaran G, Varadarajan K N and Krishnan S 2018 Exhaust System Muffler Volume Optimization of Light Commercial Vehicle Using CFD Simulation *Materials Today: Proceedings* vol 5 (Elsevier) pp 8471–9
- [18] Vishwakarma A, Chandramouli P and Ganesan V 2009 Acoustic Analysis of Exhaust Muffler of a 4-Stroke Engine *SAE Int. J. Passeng. Cars – Mech. Syst.* **2** 1303–11